Simulation of Flux Density in a Hybrid Coil Superconducting Magnetic Energy Storage Using COMSOL Multiphysics

S. Roy[*1], G. Konar[1]
[1]Jadavpur University Power Engineering Department, Kolkata, West Bengal, India
*Address of corresponding author: LB-8, Sector-III, Salt Lake, Kolkata-700098, India
*Email-id of corresponding author: satrajit.roy.86@gmail.com

Abstract: Energy storage is indispensable for hybrid power systems using non-conventional resources. Technologies like batteries, compressed air energy storage (CAES), pumped hydro plants etc. generally have associated energy losses and time delay during energy conversion process. However, there is no energy loss when a Superconducting Magnetic Energy Storage (SMES) unit converts electrical energy stored in the form of magnetic energy. Low Temperature Superconducting (LTS) toroids and solenoids were already in use. Presently, first and second generation High Temperature Superconducting (HTS) coils are used either independently (for energy storage) or with LTS coils in a hybrid mode (for particle accelerators). Prototypes of few hybrid coils normally made of BSCCO and NbTi/Nb_3Sn have been designed and tested. This work involves 3D simulation of the magnetic field distribution of such a hybrid coil using COMSOL Multiphysics. Simulated field profile agrees with published test results of similar coil. Field falls from 7.5 T (inner wall of HTS coil) to 0.04 T outside the coils.

Keywords: Hybrid coil, SMES, HTS and LTS.

1. Introduction

Today a vast majority of electrical energy is being generated by burning fossil fuels in the thermal power plant. Although coal fired plants render themselves particularly useful in meeting the base load yet one major concern is that these resources are getting depleted day by day. For this reason non-conventional power resources are employed to harness energy in addition to the conventional methods. One major demerit of electrical energy is that it is difficult to store it for a very long period economically. Only in case of grid-connected systems the excess energy can be properly used as and when required. But for any standalone type of system energy storage is a must otherwise excess energy may have to be dumped. Present researches and studies have provided us with a few options to achieve the storage of energy but the economic feasibility is yet to be examined. These options are primarily classified as direct storage (examples are super-capacitors and batteries) and indirect storage (examples are pumped hydro plants, flywheel energy storage, compressed air energy storage-CAES etc.) [1-3]. SMES is an example of direct energy storage.

A Superconducting Magnetic Energy Storage (SMES) system stores the energy in its magnetic field produced by the direct current flowing through a coil made of superconducting materials like NbTi/Nb_3Sn. Liquid He is used as the cryogenic material for these low temperature superconductors [4]. A typical SMES system includes four parts - the superconducting coil (SC), the power conditioning system (PCS), the cryogenically cooled refrigerator or the cryogenic system (CS) and the cooling unit (CU) [5]. Since superconductors practically offer almost no resistance to current flow energy can be stored indefinitely in the magnetic field owing to the reason that the direct current will not decay once the coil has current flowing through it and that the stored energy can be supplied to the network by discharging the same coil. The power conditioning system comprises an inverter or rectifier circuit to transform AC power to DC or convert DC back to AC power. The employing of these power electronic switches causes a very small fraction of energy loss for both the directions of operation. SMES loses the least amount of electricity in the energy storage process compared to other methods of storing energy because in the other methods, energy conversion processes from electrical to mechanical (flywheel energy storage) or from electrical to chemical (batteries) are involved whereas in SMES electrical energy is directly stored in the magnetic field. SMES systems are thus quite highly efficient [6].

Superconductivity can be exhibited by materials like NbTi (niobium-titanium) at a very low temperature of 4.2 K which is known as low temperature superconductivity (LTS) or it can be exhibited at relatively higher temperatures (77 K)

by materials like Bi-2212 (bismuth-strontium-calcium-copper oxide or BSCCO-2212) and Bi-2223 (BSCCO-2223), the phenomenon being known as high temperature superconductivity (HTS). The low temperature superconductors can be placed in a copper matrix and the high temperature superconductors can be placed in silver matrix to provide support and thermal stability [6,7]. The emergence of LTS marked the first significant application of SMES as an energy storage device in the form of LTS SMES [8-11]. However, with the advent of time not only magnetic storage but also various other applications like active-reactive power control, output power fluctuation stabilisation etc. have been possible [12]. The use of HTS in SMES involves liquid nitrogen as cryogen which in turn reduces the cost of refrigeration [13]. Very high magnetic field can be produced using either LTS coils [14] (**Figure 1**) or hybrid HTS – LTS coils which finds application in particle accelerator projects [15]. Hybrid coil concept was developed as a part of the Japanese Development of Superconducting Power Network Control Technology [16-18].

Few experimental works on hybrid coil design and testing of the prototype have been performed [15,16]. But finite element simulation of field distribution of such a hybrid coil [16] is yet not reported. This work involves the simulation of the flux density distribution of a hybrid coil employing both HTS and LTS coils. The descriptions of the coil and design parameters are presented in the following section.

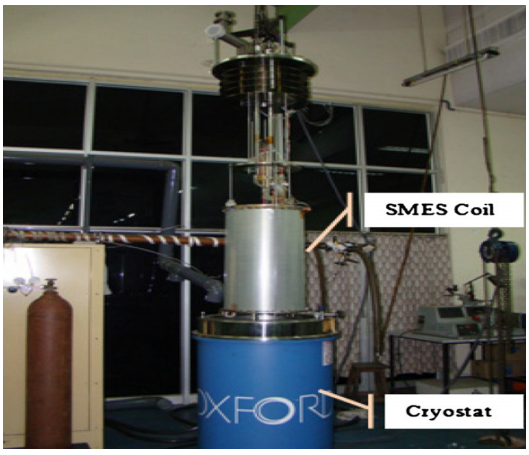

Figure 1: Photograph of an SMES used in Variable Energy Cyclotron Centre (VECC), India [14].

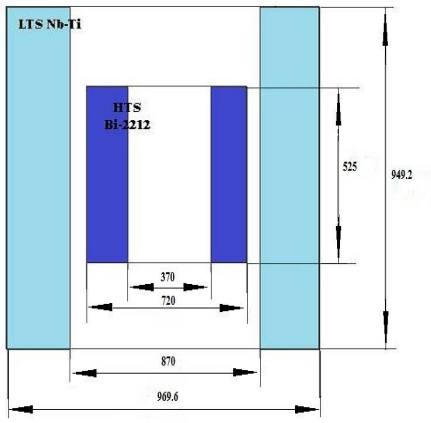

Figure 2: Schematic diagram of the hybrid coil longitudinal section.

2. Coil Design

Our modelling activity comprised the simulation of flux density of a typical SMES cylindrical hybrid-coil whose outer coil is made of LTS Nb-Ti (niobium-titanium) and the insert coil is made of HTS Bi-2212 material. The schematic diagram of the coil structure is shown in **Figure 2**.

Here the width of the HTS Bi-2212 insert coil tape is chosen to be 13.5 mm and the thickness is 1.6 mm. The insulation used in between turns is of laminated polyimide of thickness 0.075 mm. The width of the outer LTS Nb-Ti coil tape is 12.36 mm and the thickness is 1.46 mm. The fibre glass insulation used in between turns and in between layers is of thickness 0.2 mm. Both the cables used are Rutherford cables. To achieve a suitable current density, the number of turns is assumed to be 100 for each of the double pancake coils and 30 for each of the single pancake coils. 16 such double pancake coils (**Figure 3**) and 70 such single pancake coils have been stacked individually to produce the HTS and LTS solenoid coils respectively. All the relevant coil dimensions and other parameters are stated in **Table 1.** Since superconductors can carry much larger current compared to conventional conductors of the same cross section, a high field can be created while consuming much less power. The current densities used for simulation are well below the critical current density values for both HTS and LTS coils.

Simulation work is done here with the help of COMSOL Multiphysics, a simulation-software.

3. Use of COMSOL Multiphysics

3.1 Physics of the Chosen Model

Table 1: Design parameters of the NbTi-Bi-2212 hybrid LTS-HTS coil

Coil	HTS	LTS
Material used	Bi-2212	NbTi
Conductor dimension, mm×mm	13.5 × 1.6	12.36 × 1.46
Type of winding	Double pancake	Single pancake
Inner diameter, mm	370	870
Outer diameter, mm	720	969.6
Coil Height, mm	525	949.2
Total no. of turns	1600	2100
Operating current, A	1655	1553
Operating temperature, K	4.2	
Peak field, T	7.5	2.4
Central Field, T	6.95	
Current Density, A/mm^2	28.820	68.993

The basic physical concept used in the modelling is that a static magnetic field is produced when direct current is passed through a solenoid. Since flux density vector ***B*** is of primary interest here and ***B*** has a relationship with the magnetic vector potential ***A*** as shown in Eqn. (3), the vector variable ***A*** is selected to be the primary variable. The model is built using the **3D Magnetic Fields** section of the **AC/DC** module. Since DC is used the **Preset Studies>Stationary option** is selected. Assuming static currents and fields, the magnetic vector potential ***A*** must satisfy the following equation:

$$\nabla \times (\mu^{-1} \nabla \times \mathbf{A}) = \mathbf{J}^e \qquad (1)$$

where μ is the permeability, and $\boldsymbol{J}^e$ denotes the externally applied current density. ***H*** is the magnetic field intensity. The relations between fields (***B*** and ***H***) and potential ***A*** are given by

$$\mathbf{B} = \nabla \times \mathbf{A} \qquad (2)$$

$$\mathbf{H} = \mu^{-1} \mathbf{B} \qquad (3)$$

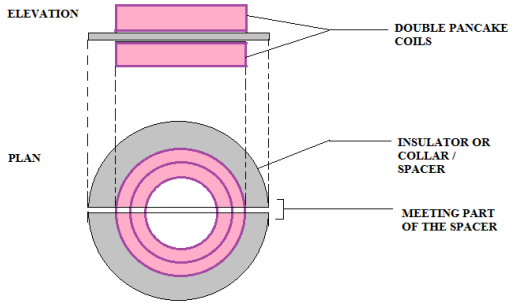

Figure 3: Structure of a single Double Pancake coil [19].

This model uses the permeability of vacuum as the medium surrounding the coil is either vacuum or air having the same magnetic permeability, that is $\mu = 4\pi \times 10^{-7}$ H/m.

3.2 Parameter Values and Equations for Simulation

The external current density is zero except in the cylindrical coils, where current densities of $J_{h,0}$ and $J_{l,0}$ are for the inner HTS coil and the outer LTS coil respectively. The internal and external current densities are used as parameters and these are defined in the **Global Definitions> Parameters** section.

Table 2: The values of current densities in the LTS and HTS coils

NAME	EXPRESSION	DESCRIPTION
J_{h0}	28.820[A/mm^2]	Current density in the HTS coil
J_{l0}	68.993[A/mm^2]	Current density in the LTS coil

The model geometry as shown **Figure 4** is built using the millimetre unit. The two coaxial coils with their corresponding dimensions are created in 3D using the **Workplane** and **Revolve** options. The medium surrounding the hybrid coil is chosen to be air because the magnetic permeability of air and that of vacuum are almost equal. For this purpose a sphere of 1000 mm radius is created around the hybrid coil. **Wireframe Rendering** (**Figure 5**) can be used to see the interiors of the model.

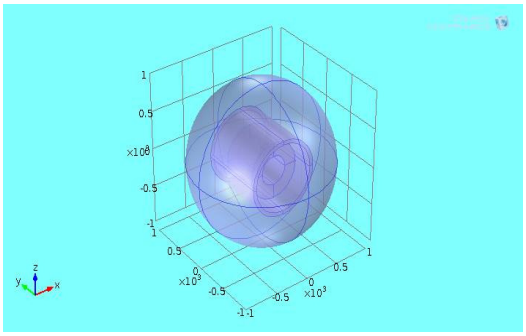

Figure 4: The model geometry.

From the **Model Builder** window by right clicking **Model** and opening the **Material Browser, Air** from the **Built-in** section is selected material of the medium surrounding the solenoid.

Ampere's Law applied to all the domains used in the model is given by

$$\nabla \times \mathbf{H} = \mathbf{J}^e \qquad (4)$$

where $\mathbf{H} = \mu^{-1}\mathbf{B}$

and $\mathbf{B} = \nabla \times \mathbf{A}$

In the External Current Density section the current density vector components are declared in the rectangular coordinates. This is done separately for both the LTS and the HTS coils respectively. These are shown in **Table 3** and **Table 4** respectively.

Table 3: Expression for current density vector components in the Cartesian coordinate for LTS coil

COMPONENTS	EXPRESSION
x	$-J_{l0} \times z/\sqrt{(x^2+z^2)}$
y	0
z	$J_{l0} \times x/\sqrt{(x^2+z^2)}$

Table 4: Expression for current density vector components in the Cartesian coordinate for HTS coil

COMPONENTS	EXPRESSION
x	$-J_{h0} \times z/\sqrt{(x^2+z^2)}$
y	0
z	$J_{h0} \times x/\sqrt{(x^2+z^2)}$

3.3 Boundary conditions

Magnetic insulation condition is applied to the entire sphere of air that surrounds the hybrid coil in

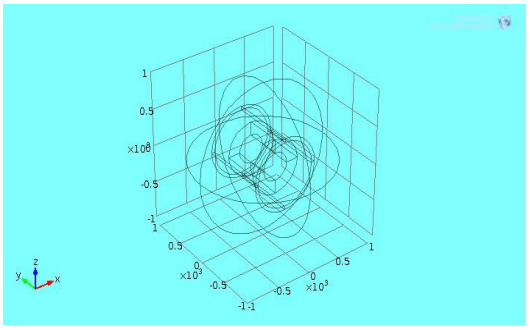

Figure 5: Model in Wireframe rendering to see its interiors.

the **Select Boundaries** section of **Magnetic Insulation**. The related equation is

$$\mathbf{n} \times \mathbf{A} = \mathbf{0} \qquad (5)$$

3.4 Meshing

Meshing is done using **Free Tetrahedral** option as the model is a 3D model. **Mesh Settings** section has the **Element Size** list from which **Coarse** is selected. Selection of Fine or Finer element size may delay the process due to huge consumption of available system memory and hence may run short of memory. In the **Size** subsection of the Free Tetrahedral, only the HTS and LTS coil domains are selected. From the **Element Size Parameters** section of Size subsection the **Maximum Element Size** is edited according to necessity and finally meshing is completed. **Figure 6** shows the mesh. The program is then executed and the simulation results thus obtained are discussed in the next section.

4. Results and Discussions

The results are finally simulated using the **3D Plot Group** option. **Arrow Volume Plot** and **Slice Plot**

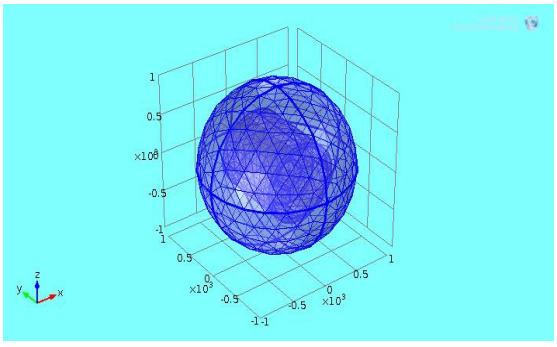

Figure 6: Meshing in 3D for hybrid coil.

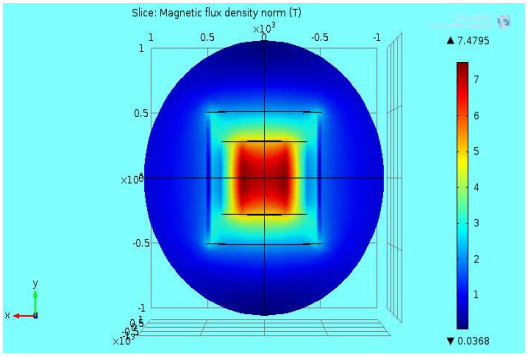

Figure 7: Slice plot depicting the flux density distribution for the hybrid coil.

options have been used for the purpose and magnetic flux distribution has been plotted in the entire simulation domain.

The simulations of the magnetic flux distribution of the hybrid solenoid are shown in **Figures 7** and **8** respectively which clearly depict the high concentration of the field in the central region of the coaxial solenoids and on the inside surface of the insert coil. The peak field is near about 7.5 T and the central field is nearly 6.95 T. The polarity of the magnet is evident from the arrow volume plot (**Figure 8**). An Excel plot of the flux density values with the *x*-coordinate has been shown in **Figure 9.** This plots the variation of the flux density values with the *x*-coordinate with fixed *y* and *z* co-ordinate values. There are two peaks at x = 160 mm and x = 429.5 mm and their respective values are B = 7.5 T and B = 2.4 T. This so happens as the maximum field is created just outside each of the two coils and decreases with the radial distance from each coil. The simulation shows that the field

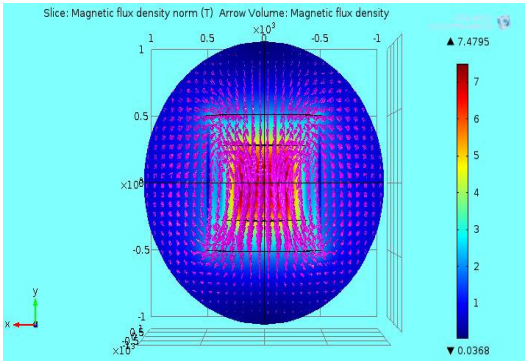

Figure 8: Arrow Volume plot for the flux density distribution of the hybrid coil.

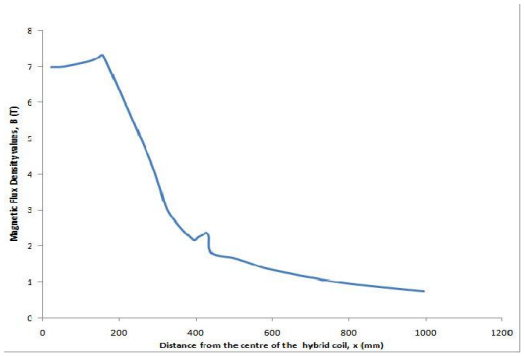

Figure 9: The graphical plot of the variation of flux density values with the *x*-distance from the centre of the hybrid coil where y = 1.53655 mm, $z = -2.27\times10^{-13}$ mm

density rapidly falls to a very low value outside the solenoid. This justifies the fact that the field density outside the coil of an infinitely long solenoid is zero.

Within the coil longitudinal cross section, the flux density falls almost linearly. In this simulation, engineering current density is considered instead of the superconductor current density whose value is always greater than the former. Hence, the simulated magnetic field distribution values will be slightly less from the actual magnetic field distribution values. However, the field profile will remain similar. The obtained flux distribution profile agrees with the published test results of similar work [16]. Also, the maximum value of the central field and the peak field depend on the current density. If current density increases both will increase. However, HTS and LTS coils of requisite increased current density should be investigated and carefully designed to increase the stored energy in a unit volume of the coil setup. This makes the size of SMES coil compact. Highly concentrated field is thus quite significant for an effective SMES.

5. Conclusions

This simulation work is based on an earlier work on hybrid coil [16]. It can be concluded that finite element simulation results are found to be agreeing with test results [16]. However, the geometry of the coil is a solenoid. Use of toroids in hybrid coil can be investigated for better performance and reduced magnetic leakage.

The discipline of hybrid coil SMES is still developing. To improve its performance several approaches can be undertaken. Out of many of such

approaches field consideration can be a suitable tool and refining the existing designs for their fields can prove to be useful in this respect. Simultaneous cost-effectiveness study is also necessary in order to ensure the economic feasibility of the project.

6. Reference

1. H.P. Tiwari & Sunil Kumar Gupta, DC energy storage schemes for DVR voltage sag mitigation system, *International Journal of Computer Theory and Engineering*, **Volume 2 (3)**, 1793-8201 (2010).
2. J.I.S. Martin, I. Zamora, J.J.S. Martin, V. Aperribay & P. Eguia, Energy storage technologies for electric applications, *International Conference on Renewable Energies and Power Quality* (2011).
3. R. Gupta, N.K. Sharma, P. Tiwari, A. Gupta, N. Nigam, A. Gupta, Application of energy storage devices in power systems, *International Journal of Engineering, Science and Technology*, **Volume 3**(1), 289 – 297 (2011).
4. M.N. Wilson, Superconducting Magnets. : Oxford University Press, 1983.
5. D. Sutanto & K.W.E. Cheng, Superconducting magnetic energy storage systems for power system applications, *Proceedings of IEEE International Conference on Applied Superconductivity & Electromagnetic Devices,* 377-380 (2009).
6. W.V. Hassenzahl, Superconducting magnetic energy storage, *Proceedings of the IEEE*, **Volume 71**(9), 1089-1098 (1983).
7. Y. Iwasa, HTS magnets: stability; protection; cryogenics; economics; current stability/protection activities at FBML, *Cryogenics,* **Volume 43**(3-5), 303-316 (2003).
8. M. Masuda & T. Shintomi, 1 MWh superconductive energy storage, *IEEE Transactions on Magnetics*, Volume 17(5), 2182-2185 (1981).
9. R.I. Schermer, H.J. Boenig, M. Henke & R.D. Turner, Conductor qualification tests for the 30-MJ Bonneville power administration SMES coil, *IEEE Transactions on Magnetics,* **Volume 17**(1), 356-359 (1981).
10. J.D. Rogers, R.I. Schermer, B.L. Miller & J.F. Hauer, 30-MJ superconducting magnetic energy storage for electric utility transmission stabilization, *Proceedings of the IEEE*, **Volume 71(**9), 1099-1107 (1983).
11. J. R. Purcell, J. D. Rogers, W.V. Hassenzahl, R. J. Lloyd & S.M. Schoenung, Coil protection for a utility scale superconducting magnetic energy storage plant, *IEEE Power Engineering Review*, 336-342 (1987).
12. M.H. Ali, B. Wu & R.A. Dougal, An overview of SMES applications in power and energy systems, *IEEE Transactions on Sustainable Energy,* **Volume 1**(1), 38-47 (2010).
13. S.M. Schoenung, W.R. Meier, R.L. Fagaly & R.B. Stephens, Design, performance and cost characteristics of high temperature superconducting magnetic energy storage, *IEEE Transactions on Energy Conversion,* **Volume 8**(1), 33-39 (1993).
14. U. Bhunia, J. Pradhan, A. Roy, V. Khare, U. Panda, A. De, S. Bandyopadhyaya, T. Bhattacharyya, S. Thakur, M. Das, S. Saha, C. Mallik & R.K. Bhandari, Design, fabrication and cryogenic testing of 0.6 MJ SMES coil, *Cryogenics* (2012).
15. Q. Wang, Y. Dai, B. Zhao, S. Song, Y. Lei, H. Wang, B. Ye, X. Hu, T. Huang, H. Wang, C. He, M. Shang, C. Wang, C. Cui, S. Zhao, Q. Zhang, Y. Diao, Y. Peng, G. Xu, F. Deng, P. Weng, G. Kuang, B. Gao, L. Lin, L. Yan, Development of high magnetic field superconducting magnet technology and applications in China, *Cryogenics,* **Volume 47,** 364-379 (2007).
16. K. Koyanagi, K. Ohsemochi. M. Takahashi, T. Kurusu, T. Tosaka, M. Ono, Y. Ishii, K. Shimada, S. Nomura, K. Kidoguchi, H. Onoda, N. Hirano & S. Nagaya, Design of a high energy-density SMES coil with Bi-2212 cables, *IEEE Transaction on Applied Superconductivity*, **Volume 16**(2), 586-589 (2006).
17. T. Tosaka, K. Koyanagi, K. Ohsemochi, M. Takahashi, Y. Ishii, M. Ono, H. Ogata, K. Nakamoto, H. Takigami, S. Nomura, K. Kidoguchi, H. Onoda, N. Hirano, and S. Nagaya, Excitation tests of prototype HTS coil with Bi-2212 cables for development of high energy-density SMES, *IEEE Transaction on Applied Superconductivity*, **Volume 17**(2), 2010-2013 (2007).
18. H. Kojima, N. Hayakawa, S. Noguchi, F. Endo, N. Hirano, S. Nagaya & H. Okubo, Thermal runaway characteristics of Bi-2212 coil for conduction-cooled SMES, *IEEE Transaction on Applied Superconductivity*, **Volume 1**(2), 1959-1962 (2007).
19. S.H. Kim, S.M. Baek, Y.S. Kim, S.Y. Chung & J.M. Joung, Surface flashover characteristics in liquid nitrogen for application of superconducting pancake coils, *Cryogenics,* **Volume 42**(6-7), 415-418 (2002).